Intelligent Viaduct Recognition and Driving Altitude Determination Using GPS Data

Li-Ta Hsu, *Member, IEEE*, Yanlei Gu, *Member, IEEE*, and Shunsuke Kamijo, *Member, IEEE*

***Abstract*—The rapid development of road networks in highly urbanized cities requires a substantial number of viaducts to reduce the increasing traffic burden on urban highways. Unfortunately, this road design deteriorates the performance of global positioning system (GPS) navigators due to the signal blockage between satellite and receiver. As a result, it is difficult for GPS navigators to determine whether the vehicle is driving on the street or viaduct. Misleading information could confuse drivers and lead them to drive irregularly, which is dangerous in heavy traffic. This paper proposes a novel classification algorithm based on the fact that different satellite signals and conditions can be observed in the on-street and on-viaduct cases by the implementation of dynamic Bayesian network (DBN) to distinguish the driving area of a vehicle. In addition, the proposed DBN can also accurately estimate the driving altitude of the vehicle according to the experiment results.**

***Index Terms*—Autonomous driving, GPS, GNSS, land application, localization, navigation, urban canyon.**

I. Introduction

GLOBAL positioning systems (GPS) play a very important role from the point of view of vehicle navigation and safety applications of intelligent transportation system (ITS). In highly developed cities, viaducts, namely, road bridges, are used to reduce the burden of traffic. Vehicle GPS navigation suffers from signal blockage under viaducts or bridges; hence, it is difficult to estimate the height of the vehicle accurately. As a result, road users experience a lot of misguidance from GPS navigators when driving in streets with viaducts, in particular in the junction of interchange between the street and viaduct [1], [2]. The misguidance could invoke unexpected driving behavior, introducing uncertainty in the traffic environment in terms of safety and traffic jams. Some Garmin models, including Nuvi 2455, 2465T, and 3790T, allow manual selection to indicate whether a driver is driving on or off the viaduct. Even though this feature can solve the problem, it also distracts the driver, leading to dangerous scenarios. There are several ways to apply sensors that distinguish whether a vehicle is on/off a viaduct and recognize elevation, e.g., active sensors such as Employee Transportation Coordinator (ETC) reader, radio-frequency identification (RFID) reader [3], [4] and passive sensors such as barometer [5], inertial navigation system (INS) [6] and camera [1], [2]. They have been proven to be effective but require additional costs [7], [8]. For current automobiles, a cost-effective solution would be a standalone GPS navigator, which consists of a GPS receiver and road map information. The objective of this paper, therefore, is to develop a new algorithm based on the information of the GPS receiver calculated position, satellite visibility and viaduct height to recognize whether the vehicle is driving on or off viaducts. The key innovative point is to use satellite visibility and pseudorange similarity as the important factors due to the characteristic of satellite blockage under viaducts.

A sequential importance resampling (SIR) particle filter (PF) integrated with dynamic Bayesian network (DBN) is proposed. The state of each particle contains the height and the recognition of an automobile on a viaduct. A logistic regression is used to train a probability model based on the satellite visibility and height of a particle. Finally, the likelihood function of each particle is decided by the pseudorange residual calculated by the receiver calculated 2D position and given height of the particle. Four typical automobile driving scenarios are tested near an urban viaduct environment: 1) under viaduct, 2) on viaduct, 3) from street to viaduct and 4) from viaduct down to street. The commercial u-blox GNSS receiver can only estimate correctly in the on viaduct case because of open-sky signal reception. In the under viaduct case, the estimated height information of u-blox is inaccurate and misleading. On the other hand, the proposed method correctly determined that the vehicle stayed under the viaduct. In the case of vehicle driving from street to viaduct, the proposed method only requires a few seconds to switch the determination from driving under to on the viaduct.

In Section II of this paper, we discuss the difficulties of conventional approaches. The developed DBN method, inferred by the particle filter, is introduced in Section III. Experiment setup and results are shown in Section IV. Finally, conclusions and implications of this study are summarized in Section V.

II. Problem Statement

This section evaluates the conventional approaches to determining whether a vehicle is driving on or off a viaduct to describe the expected problems to be solved. Two kinds of conventional approach, general GPS positioning methods and map matching, are discussed.

Manuscript received March 6, 2017; revised June 9, 2017, July 6, 2017, and July 30, 2017; accepted July 31, 2017. Date of publication August 9, 2017; date of current version October 31, 2017. *(Corresponding author: Yanlei Gu.)*

L.-T. Hsu is with the Hong Kong Polytechnic University, Hung Hom, Hong Kong (e-mail: lt.hsu@polyu.edu.hk).

Y. Gu and S. Kamijo are with the University of Tokyo, Tokyo 153-8505, Japan (e-mail: guyanlei@kmj.iis.u-tokyo.ac.jp; kamijo@iis.u-tokyo.ac.jp).

Color versions of one or more of the figures in this paper are available online at http://ieeexplore.ieee.org.

Digital Object Identifier 10.1109/TIV.2017.2737325

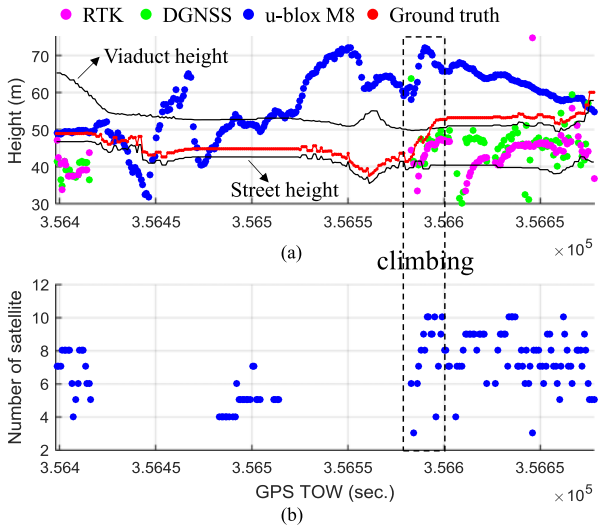

Fig. 1. (a) Estimated altitude by GNSS receiver (u-blox M8) and applying its measurement based on DGNSS and RTK techniques. (b) The number of satellites received by the GNSS receiver.

A. *Performance of Conventional GPS Approaches*

An intuitive approach to determine automobile driving on/off viaduct is to obtain the estimated altitude by GPS receiver. If it is higher than the height of the viaduct, then the vehicle is very likely to be on top of it and vice versa. A test drive starting from the street and climbing to the viaduct is conducted in an urban canyon in Tokyo. The results of a consumer-level GNSS receiver applied with well-known GPS argumentation methods are shown in Fig. 1. The differential GNSS (DGNSS) [9] and real-time kinematic (RTK) [10] cannot output a single point solution in most of the period while driving in the street because of a lack of received satellites. After the climb to the viaduct, the number of received satellites increased, and both GPS methods were then capable of outputting an altitude solution. As shown at the top of Fig. 1, their accuracies do not satisfy the need to distinguish the vehicle location. The GPS receiver usually implements sophisticated filters so that it can always provide localization service [11]. Its altitude estimation is not accurate enough to be a distinctive hint. In fact, GPS positioning theory is deficient in altitude estimation due to the limited satellite distribution in elevation direction as shown in Fig. 2. This characteristic results in the vertical dilution of precision (V-DOP) usually being higher than the horizontal DOP (H-DOP) [12]. In other words, localization accuracy in the vertical is worse than that in the horizontal. An observation from the bottom panel of Fig. 1 is that the number of satellites received is highly correlated with driving altitude since the viaduct will easily block the line-of-sight (LOS) transmission path between the satellite and vehicles driving on the street. This research is inspired by this observation and further derives an on/under viaduct scenario recognition algorithm.

B. *Map Matching*

General map matching (MM) algorithm matches the localization solution provided by the GPS receiver on a 2-dimensional

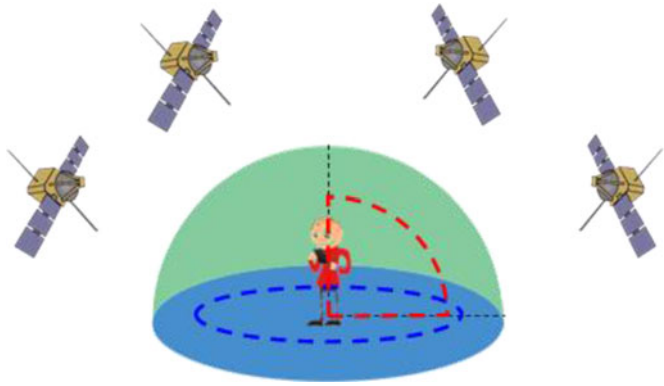

Fig. 2. Demonstration of geometric defection in vertical estimation of GPS positioning. The available degree in horizontal (blue) and vertical (red) directions are 360 and 90, respectively.

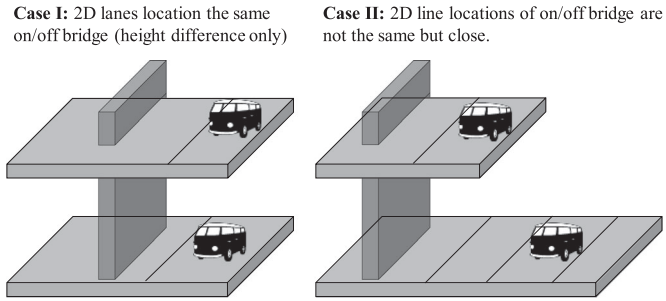

Fig. 3. Illustration of two difficult cases using map matching to recognize the altitude of automobile.

(2D) map. Inaccurate solutions, such as points inside buildings, can be discarded. In addition, the estimated vehicle trajectory can be shaped according to the road map. Intuitively, this is achieved by comparing the solution points with the nearest segment. This is proven effective for improvement of GPS localization accuracy [13]–[16]. However, there are two difficult cases for MM even if assuming the 2D localization result provided by GPS is accurate. They are illustrated in Fig. 3.

In Case I, the MM algorithm will be difficult to determine if no destination information is provided [17]. Case II requires the 2D maps to provide the location of multiple lanes within a street. A lane-level map matching with the aid of vision sensor was proposed [18]. In 2014, a highly detailed map designed for autonomous driving was introduced, known as the *lanelet* map [19]. Based on the particular map design, a new lane-level map matching based on the path hypothesis of the vehicle was proposed [20]. However, a large amount of time is still necessary to prepare the highly detailed 2D maps. For example, currently, the map provided by *OpenStreetMap* (OSM) [21] in our test field is insufficient to perform the lane-level map matching. Based on the reasons above, the map matching algorithm is not considered in this work.

Research of 3D map matching using GPS and enhanced detail of 3D digital map is a promising approach to improve urban GPS localization [22]–[24]. GNSS shadow matching, which is one of the most famous 3D mapping aided (3DMA) GNSS localization methods, makes use of a 3D building model to generate building boundaries to predict satellite visibility [25], [26]. Its application

in land vehicle localization is discussed and improved in [27]. Instead of excluding the GNSS multipath and non-line-of-sight (NLOS) effects, many studies use the ray-tracing simulation and 3D building model to estimate the reflection length of the GPS signal and further improve localization accuracy [28]–[30]. This pseudorange-based 3DMA GNSS method is finally improved to a performance with a localization accuracy of less than 3 meters in the across-street direction even in highly urbanized areas [31], [32]. However, all of the listed studies focus on the estimation of the horizontal position. The vertical position of the vehicle is usually assumed as the summation of the elevation and vehicle height, as the 3DMA GNSS is usually implemented by hypothesis-based estimation methods such as particle filter. Thus, the computation load of 3-dimensional particles is excessive [33]. In addition, 3D mapping of urban viaducts is too complex for current 3DMA methods. As a result, the application of 3DMA in the estimation of vehicle altitude remains open.

III. Dynamic Bayesian Network (DBN)

In this paper, not only is vehicle on/under bridge estimated but also the altitude of the vehicle. This requirement implies that both discrete and continuous states are required to be estimated. In general, the discrete state can be classified by the hidden Markov model (HMM). The continuous states are usually estimated by linear dynamic systems (LDS), such as Kalman filtering. In fact, both HMM and Kalman filter can be regarded as a simple form of dynamic Bayesian network (DBN) with proper assumptions. A complex DBN is therefore able to combine a HMM with a LDS, which is used in this study [34]. The random variable that is used as the states of the proposed DBN is introduced as follows.

H: Vehicle driving height (altitude) above mean sea level.

B: Decision of vehicle driving on/under bridge (viaduct). This paper assumes that the vehicle is driving on or under a bridge, and the climb to the bridge is neglected.

$$B_t \in \{\text{on}, \text{under}\} \tag{1}$$

SV: GNSS satellite visibility of vehicle. The definition of satellite visibility is the number of acquired satellites dividing the expected number of satellites in view. Value 0 indicates that no satellites are visible to the receiver, implying the vehicle is likely to be in an indoor area. The expected position of the satellite can be estimated by the broadcast almanac [35].

$$SV_t \in [0, 1] \tag{2}$$

X: Horizontal position of vehicle provided by receiver.

$$\boldsymbol{X_t} = \begin{bmatrix} x_t^{lat} \\ x_t^{lon} \end{bmatrix} \tag{3}$$

Sp: Speed of vehicle provided by receiver.

PR: Pseudorange measurements provided by receiver. ρ denotes the pseudorange, which consists of the LOS distance, delays and receiver clock bias. *j* denotes the number of satellites received at time *t*.

$$\boldsymbol{PR}_t = \left\{ \rho_t^1 \dots \rho_t^j \right\}^T \tag{4}$$

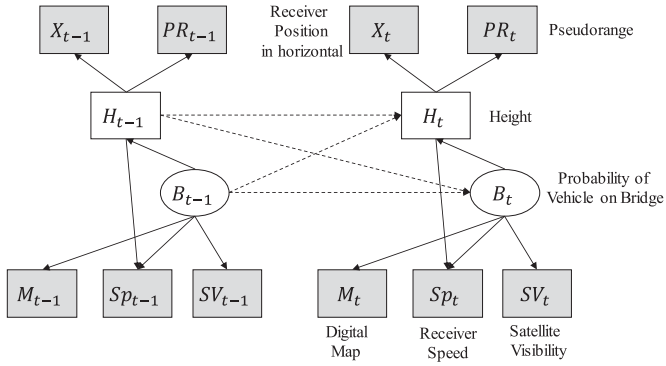

Fig. 4. Proposed two-slices DBN model. The rectangular and round shapes denote the continuous and discrete values, respectively. The solid and dash lines denote intra-temporal and inter-temporal causal edges, respectively. The shaded rectangular shapes denote either observation ($\boldsymbol{PR_t}, \boldsymbol{X_t}$) or context information (SV_t, M_t, Sp_t).

M: Heights of bridge and street provided by digital map. This paper assumes the heights of the street and bridge (viaduct) are available in the future navigator. The received calculated position is used to find the bridge height close to the vehicle position. The heights are also in mean sea level.

$$\boldsymbol{M_t} = Map\left(\boldsymbol{X_t}\right) = \begin{bmatrix} h_t^{\text{bridge}} \\ h_t^{\text{street}} \end{bmatrix} \tag{5}$$

The overview (dependency graph) of the proposed DBN is given in Fig. 4.

The designed state transition model can be summarized as:

$$\begin{aligned} &P\left(B_t, H_t | SV_t, M_t, Sp_t, B_{t-1}, H_{t-1}\right) \\ &= P\left(B_t | SV_t, M_t, Sp_t, H_{t-1}, B_{t-1}\right) \times P\left(H_t | B_t, B_{t-1}, H_{t-1}\right) \end{aligned} \tag{6}$$

The on/under viaduct model $P(B_t|SV_t, M_t, Sp_t, H_{t-1}, B_{t-1})$ and dynamic model $P(H_t|B_t, B_{t-1}, H_{t-1}, Sp_t)$ will be introduced in Sections III-A and III-B, respectively. The observation model is represented as $P(\boldsymbol{PR_t}|\boldsymbol{X_t}, H_t)$, which will be introduced in Section III-C. Finally, the inference of the DBN is given in the last sub-section.

A. Vehicle On-Under Viaduct Determination Model

This model is inspired from the fact that satellite visibility has strong correlation with the driving area of a vehicle as shown in the bottom panel of Fig. 1. The definition of satellite visibility is the number of acquired satellites dividing the expected number of satellites in view as (7).

$$SV = \frac{\text{number of SV received}}{\{SV \text{ by almanac} | el > 10^o\}} \tag{7}$$

The expected number of satellites can be calculated by predicting the satellite position using the almanac attached in the satellite navigation data [35]. In a general setting, satellites with an elevation angle, *el*, less than 10 degrees will not be used in the positioning process. It is important to note the number of acquired satellites, and the received signal strength could be affected by the dynamics of the receiver, as noted by [11], [36],

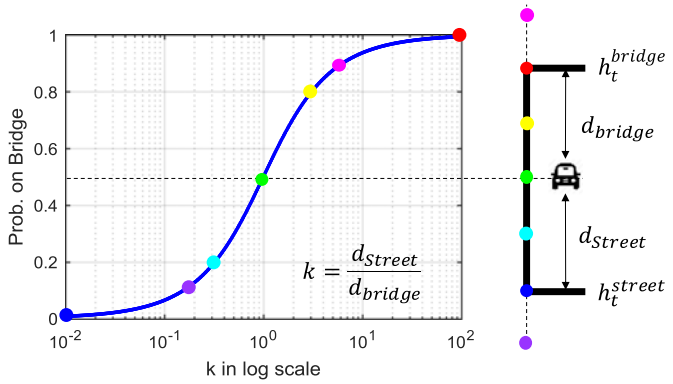

Fig. 5. Illustration of the proposed probabilistic model based on the ratio of the vehicle altitude in bridge and street.

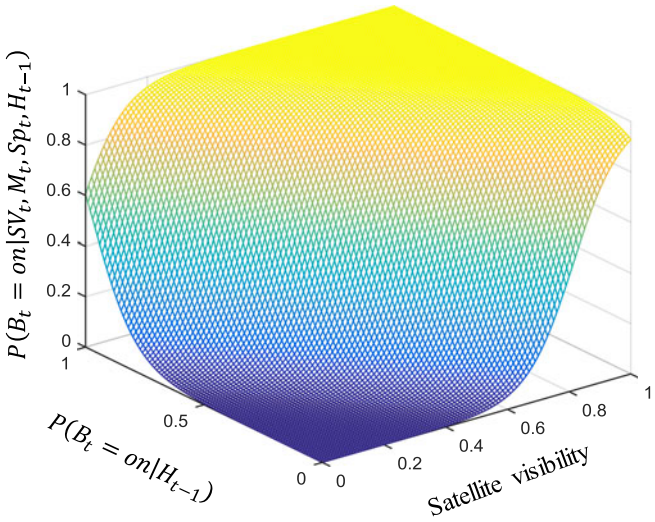

Fig. 6. Visualization of the trained vehicle on-under bridge determination model.

[37]. The reflected signals, also well-known NLOS, will continuously affect the signal acquisition and tracking processes [38]. Thus, the velocity of the receiver must be used as indication to separate the model into dynamic and static cases [39].

In addition to satellite visibility, the estimated altitude of the vehicle is also essential for the algorithm to make the decision. A probabilistic model of vehicle on bridge based on the vehicle height is proposed, and its idea is illustrated in Fig. 5. If the estimated altitude is in the middle, i.e., right between the street and bridge (the green dot on the right of Fig. 5), the probability of vehicle on bridge should be 50%.

If the estimated altitude is the altitude of the bridge, the probability of vehicle on bridge should be 100%. If a ridiculous altitude is estimated – for instance, a very high altitude could lead to $d_{\text{bridge}} \approx d_{\text{street}}$ – the probability of vehicle on bridge is about 50%. The probabilistic model can be expressed as:

$$P\left(B_t = on|H_{t-1}\right) = \frac{2}{\pi}\tan^{-1}\left(\frac{\left|h_t^{\text{bridge}} - H_{t-1}\right|}{\left|h_t^{\text{street}} - H_{t-1}\right|}\right) \tag{8}$$

Both the satellite visibility and probabilistic model of vehicle on bridge are considered as essential factors; hence, they are used in a binominal logistical regression to train the decision model [40]. The training datasets are collected under a scenario where the vehicle drives from the street and climbs to the bridge. The $P(B_t = on)$ is labelled as 0 or 1 while the vehicle is under or on bridge, respectively. The data during the climb are excluded from the dataset because of the difficulty of labelling a true $P(B_t = on)$. The model is shown in (9) and visualized in Fig. 6. The data for satellite visibility and ground truth altitude are collected and labelled with the correct decisions.

$$P\left(B_t = on|SV_t, M_t, Sp_t, H_{t-1}\right) = \begin{cases} \dfrac{exp\left(L\left(SV_t, P\left(B_t = on|H_{t-1}\right)\right)\right)}{1 + exp\left(L\left(SV_t, P\left(B_t = on|H_{t-1}\right)\right)\right)}, & Sp_t > \eta \\ P\left(B_{t-1} = on|SV_{t-1}, M_{t-1}, Sp_{t-1}, H_{t-2}\right), & \text{otherwise} \end{cases} \tag{9}$$

$$P\left(B_t = \text{under}\right) = 1 - P\left(B_t = on\right) \tag{10}$$

where η denotes a pre-defined velocity threshold to determine whether the vehicle is moving or stopping. If the vehicle is stopping, the model remains the same value as in the previous epoch. This papers adopts 1.5 meters per second as the threshold based on the rule of thumb. L is a linear function of influential factors.

$$L\left(SV_t, P\left(B_t|H_{t-1}\right)\right) = \beta_1 + \beta_2 SV_t + \beta_3 P\left(B_t|H_{t-1}\right) \tag{11}$$

where β_0, β_1 and β_2 are -11.1, 13.6 and 11.5, respectively. The trained model while the vehicle is in dynamic mode is shown in Fig. 6. As can be seen, the higher the satellite visibility that is obtained, the higher the probability that the vehicle is driving on the bridge.

B. State Transition Model

For reasons of simplicity, $P(B_t = on)$ is used to denote $P(B_t = on|SV_t, M_t, Sp_t, H_{t-1})$ in this sub-section. A moving average (MA) model is applied to describe the transition of the decision model since the vehicle will not suddenly jump onto a bridge, which is expressed as:

$$P\left(B_t = on|B_{t-1} = on\right) = \frac{1}{\kappa} P\left(B_t = on\right) + \frac{\kappa - 1}{\kappa} P\left(B_{t-1} = on\right) \tag{12}$$

where κ denotes the order of the MA model, and a second-order model is used heuristically. It is important to note that the decision of a vehicle on a bridge can reveal the height of a vehicle. In addition, based on the fact that the vehicle only drives on streets and bridges rather than at ridiculous heights, a linearized equation can be expressed as shown below:

$$H_t^{P(B_t = on)} = h_t^{\text{street}} + P\left(B_t = on\right) \cdot \left(h_t^{\text{bridge}} - h_t^{\text{street}}\right) \tag{13}$$

Again, an MA model is used to represent the relationship from the state decision B to state height H as below.

$$H_t = \frac{1}{\kappa} H_t^{P(B_t=on)} + \frac{\kappa - 1}{\kappa} H_{t-1} \tag{14}$$

C. Observation Model

There are two common levels of GPS observation, and they can be formatted as NMEA and RINEX. NMEA data contain the information of the number of the received satellite and 3D position and the velocity of the automobile estimated by the GNSS receiver. RINEX data include raw pseudorange, Doppler shift and carrier phase measurements of each acquired GNSS signal. For the proposed method, there are two reasons that RINEX is more beneficial than NMEA. First, the localization result from NMEA is estimated by the GPS receiver itself, which is implemented with a strong but ambiguous filtering technique. This filtering technique will lead the multipath effects of previous epochs also affecting the current one. Therefore, the NMEA-based observation model cannot fully represent the likelihood function of the current epochs. On the other hand, RINEX provides the pseudorange for an epoch by epoch positioning; hence, it can better estimate the likelihood function of the observation model. Second, the pseudorange measurements can be evaluated using the idea of a consistency check. As indicated by [41], the pseudorange residue can be regarded as an evaluation index of the consistency between all the measurements.

Using RINEX level GPS data, the general least square using pseudorange measurement is applied to estimate the receiver position, and clock bias is shown in (15).

$$\boldsymbol{PR_t} = \boldsymbol{G}\boldsymbol{X_t} + \omega_t, \;\; \omega \in N(0, \sigma_\omega) \tag{15}$$

where ω denotes a zero-mean Gaussian noise and $\boldsymbol{G}$ denotes the observation matrix consisting of the unit line of sight (LOS) vector between the satellite and receiver positons, which is:

$$\boldsymbol{G} = \begin{bmatrix} a_{lat,1} & a_{lon,1} & a_{alt,1} & 1 \\ \vdots & \vdots & \vdots & \vdots \\ a_{lat,j} & a_{lon,j} & a_{alt,j} & 1 \end{bmatrix} \tag{16}$$

where $a_{e,1}$ denotes a unit LOS vector between the receiver and the 1st satellite. The fourth column of $\boldsymbol{G}$ is 1 because all the pseudorange measurements share the identical receiver clock bias [12]. This paper assumes that the consumer-level GNSS receiver-estimated horizontal position is relatively more accurate than the height because of the characteristic of satellite geometry mentioned earlier. Thus, the estimated horizontal position and the height predicted by the dynamic model are applied to (15); as a result, the receiver clock bias is the only unknown to be estimated as (17).

$$\boldsymbol{b_t} = \begin{bmatrix} \rho_{1,t} \\ \vdots \\ \rho_{j,t} \end{bmatrix} - \begin{bmatrix} a_{lat,1} & a_{lon,1} & a_{alt,1} \\ \vdots & \vdots & \vdots \\ a_{lat,j} & a_{lon,j} & a_{alt,j} \end{bmatrix} \begin{bmatrix} x_t^{lat} \\ x_t^{lon} \\ H_t \end{bmatrix} \tag{17}$$

Hence, the pseudorange residue can also be calculated by:

$$\hat{\boldsymbol{\varepsilon}} = \boldsymbol{PR_t} - \begin{bmatrix} a_{lat,1} & a_{lon,1} & a_{alt,1} \\ \vdots & \vdots & \vdots \\ a_{lat,j} & a_{lon,j} & a_{alt,j} \end{bmatrix} \begin{bmatrix} x_t^{lat} \\ x_t^{lon} \\ H_t \end{bmatrix} - \hat{\boldsymbol{b}}_{\boldsymbol{t}} \tag{18}$$

Finally, the sum of square error (SSE) can be calculated as (19) to indicate the bias of normal distribution model.

$$SSE = \hat{\boldsymbol{\varepsilon}}^{\boldsymbol{T}} \hat{\boldsymbol{\varepsilon}} \tag{19}$$

Thus, the observation model can be written as:

$$P(\boldsymbol{PR_t}|\boldsymbol{X_t}, H_t) = N(SSE, \sigma_\omega) \tag{20}$$

However, if the pseudorange measurement is not available from the GPS navigator, the NMEA level of measurement will be used instead. In that case, the observation model is modelled using the difference between the particle height and receiver estimated height. Thus, the observation became:

$$P(\boldsymbol{PR_t}|\boldsymbol{X_t}, H_t) = N(|H_t - H_t^{rcv}|, \sigma_H) \tag{21}$$

where σ_H denotes the noise of the height estimation of the GPS navigator.

D. Inference of DBN by Particle Filter

A sample-based estimation method, particle filter (PF), is used to infer the states. Particularly, a sequential importance resampling (SIR) particle filter is selected due to the assumption that the prior probability distribution is distributed as an importance function [42]. The weighting of the particle can be denoted as:

$$w_t^i \approx w_{t-1}^i P\left(\boldsymbol{PR_t}|\boldsymbol{X_t}, H_t^{(i)}\right) \tag{22}$$

The weight average of the height and probability of vehicle on bridge can be determined.

$$\begin{aligned} P(B_t) = & \sum_{i=1}^{n} P\left(B_t, H_t^{(i)}|SV_t, M_t, Sp_t, B_{t-1}, H_{t-1}^{(i)}\right) \\ & \times w_{t-1}^i P\left(\boldsymbol{PR_t}|\boldsymbol{X_t}, H_t^{(i)}\right) \end{aligned} \tag{23}$$

Finally, the posterior probability can be obtained using (23). It will be used to indicate that the vehicle is driving on the bridge if the posterior probability is larger than 0.5.

IV. Experiment Results

A. Experiment Setup

The experiments took place in the Shinjuku area of Tokyo, Japan. The environments of on and under viaduct are illustrated in Fig. 7. Four driving scenarios are tested:

1) keep driving on the bridge
2) keep driving in the street (under bridge)
3) driving from the street and climbing up to the bridge and
4) driving from the bridge and descend to the street.

A consumer-grade GNSS receiver, u-blox M8N evaluation kit, is used to record RINEX [43] and NMEA [44] data. Aerial point cloud data are purchased to provide the altitude of viaduct

Fig. 7. Tested environment in Tokyo, Japan (courtesy of Google Street View).

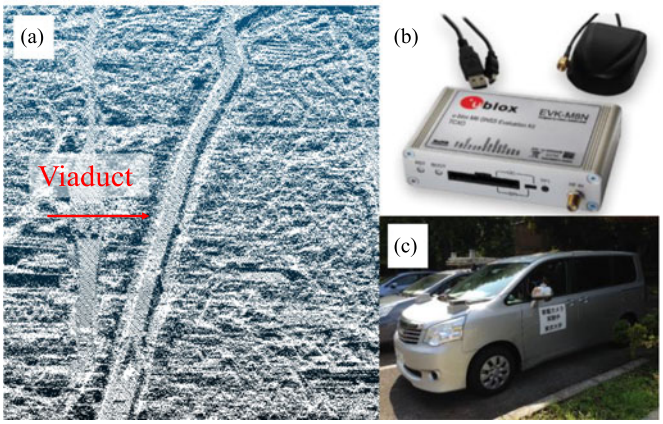

Fig. 8. Experiment setup. (a) aerial point cloud data, (b) consumer-grade GNSS receiver and (c) automobile used in the data collection.

and street because they are not provided in the OSM. They are shown in Fig. 8. The patch antenna is attached to the top of the automobile. A camera synchronized with a GPS receiver is equipped to label whether an automobile is actually driving on a street or bridge. The dates of data collection are 18th February and 23rd May 2016. The first group of data are used to train the model as shown in Fig. 6. The second group of data are used to evaluate the proposed method. Four methods are tested, each of which apply different levels of information:

1) HMM estimation considering satellite visibility (SV)
2) HMM estimation considering height estimated by the GNSS receiver
3) Proposed method (DBN+PF) using SV and NMEA
4) Proposed method (DBN+PF) using SV, NMEA and RINEX.

There are five particles equally distributed from 0 to 100 meters in Methods 3 and 4.

B. Evaluation of Height and Viaduct Recognition

The results of Scenario 1, 2, 3 and 4 are shown in Figs. 9, 10, 11 and 12, respectively. The x-axis of both top and bottom panels is GPS time in units of seconds. The y-axis of the top panel is the probability of the decision of vehicle driving on bridge, namely, $P(B_t = on)$. The ground truth of recognition is labelled by observing the video that is recorded. The y-axis of the bottom panel is the driving altitude of an automobile estimated by different methods. The block dash line denotes the height of the street and bridge. The ground truth of driving

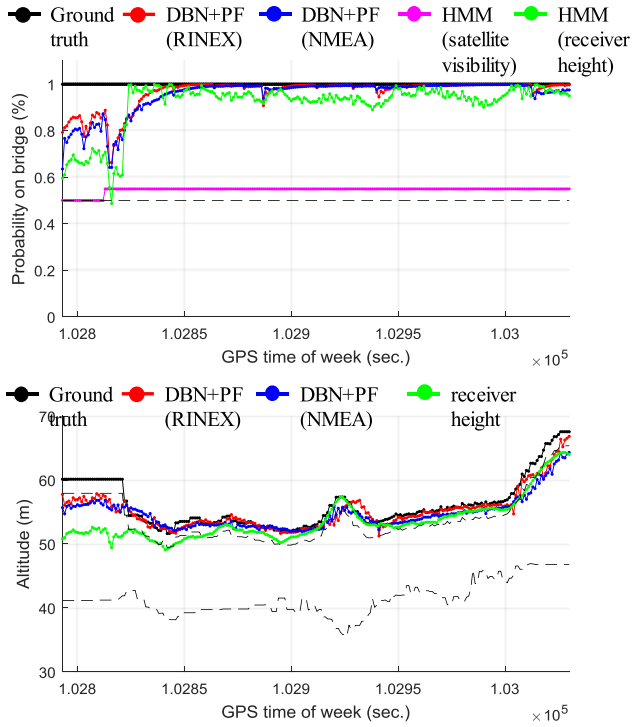

Fig. 9. Result of test Scenario 1, vehicle keeps driving on bridge.

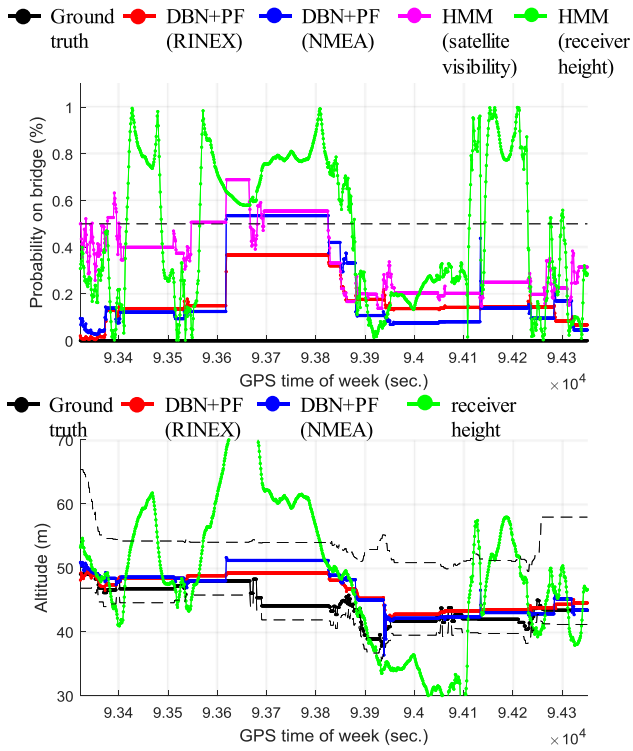

Fig. 10. Result of test Scenario 2, vehicle keep driving on street.

altitude is labelled by adding the street/bridge height with the height of the automobile (about 2.1 meters).

In the scenario of driving on bridge, as can be seen from the bottom panel of Fig. 9, the GNSS receiver can accurately determine the driving height of the automobile (green line) most of

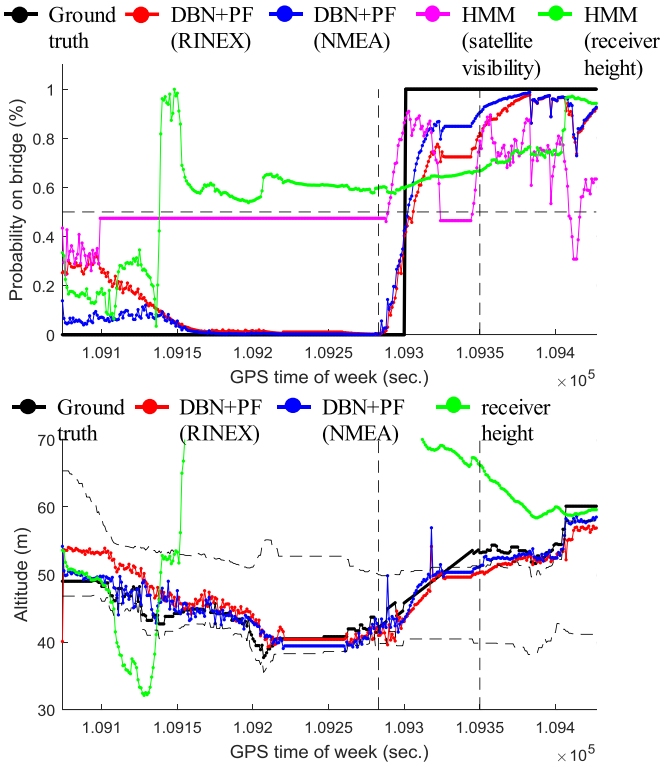

Fig. 11. Result of test Scenario 3, vehicle drives from street and climbs to bridge.

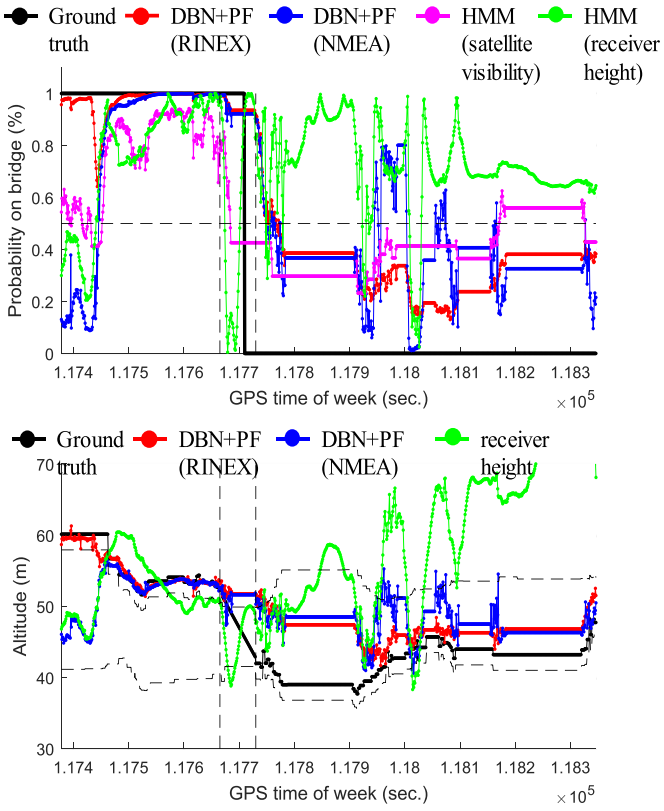

Fig. 12. Result of test Scenario 4, vehicle drives from bridge and descends to street.

the time. The number of receivable GNSS signals is sufficient because the signal reception on the bridge is much healthier than the reception under the bridge. Therefore, both HMM using the receiver-calculated height or SV can also successfully recognize that the vehicle is driving on the bridge. The two DBN methods also accurately estimate the driving altitude and correctly recognize that the vehicle is driving on the bridge after few iterations.

The result of Scenario 2 is shown in Fig. 10. As shown in the bottom panel of Fig. 10, the altitude estimated by the GNSS receiver is fluctuating and very unstable. Accordingly, the HMM using the receiver-estimated height cannot correctly determine whether the vehicle is driving on the street or bridge. Interestingly, HMM using SV can roughly indicate that it is driving on the street, excepting the middle part of the figure. The vehicle stopped at the intersection several times during the test; hence, the satellite visibility becomes unreliable as mentioned in the methodology Section. At these particular periods, the trained vehicle on-under bridge determination model (as visualized in Fig. 6) will not be used in DBN+PF-based methods. The states of the particle, $P(B_t = on)$ and H_t, will remain the same as those in the previous epoch because the vehicle is stopping. However, DBN based on NMEA data and SV also still falsely recognizes the driving status in the middle part; both the receiver-estimated height and SV are giving erroneous indication in this middle part. DBN using RINEX data can avoid faulty recognition. This method gives proper weight to each particle based on the *SSE* of the pseudorange residual as shown in (19). As a result, the particle with lower altitude is given a higher weight compared with the particle with higher altitude. Thus, the method can make the correct recognition.

The result of Scenario 3 is shown in Fig. 11. The automobile drives on the street then climbs to the bridge. As shown in the top panel of Fig. 11, HMM using receiver height incorrectly estimates that the vehicle climbs to the bridge about 4 minutes earlier. Again, HMM using SV can roughly recognize where the vehicle drives. Both DBN methods are also capable of recognizing the driving status and accurately estimating the driving altitude. The DBN methods are inferred by the SIR particle filter. The height H_t of particles is propagated based on the $P(B_{t-1} = on)$, which is strongly correlated with satellite visibility.

As a result, both DBN-based methods achieve satisfactory results. It is interesting to note the duration of climbing, which is indicated as the vertical dashed lines in Fig. 11. The proposed DBN methods only delay a few seconds to correctly determine that the vehicle is climbing onto the bridge.

The performance of the scenario of driving from the bridge and descending to the street is similar to the previous scenario. When the vehicle descends to the street, the vehicle drives very slowly because of a traffic jam. In this case, the pre-defined velocity threshold cannot fully indicate whether the automotive motion is stopping or moving. As a result, states $P(B_t = on)$ and H_t of the particle remain the same during the descent. DBN methods therefore require more time to successfully recognize that the vehicle is descending from the bridge. Although there

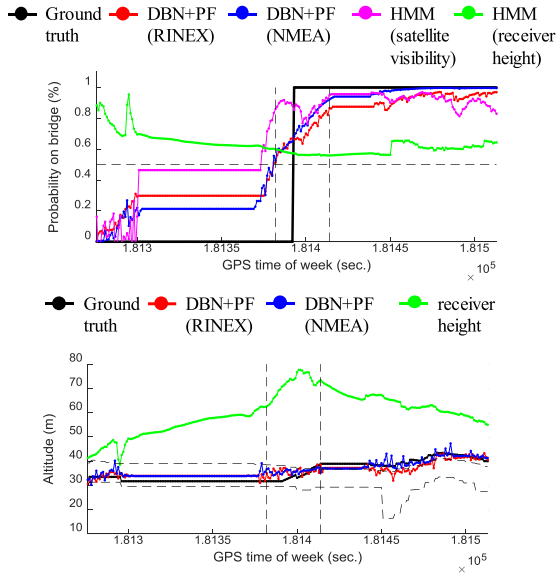

Fig. 13. Result of test Scenario 3, vehicle drives from bridge and descends to street in second experiment area.

is a delay in recognizing the transition from bridge to street, the proposed system maintains high stability in both the on- and off-bridge periods.

C. Evaluation of Height and Viaduct Recognition at Second Experiment Area

In order to show the effectiveness and generalizability of the proposed model, an additional experiment in a different area of Tokyo is conducted. The result of the scenario of climbing from street to bridge is shown in Fig. 13. As can be seen, the height estimated by the GNSS receiver suggested that the vehicle kept driving on the bridge. Satellite visibility can indicate whether the vehicle is driving on or under the bridge. As a result, both DBN methods are also capable of determining the height of the vehicle. It is important to note that the proposed model is effective in the different viaduct areas in Tokyo. However, if the sounding area of a viaduct is not as high (i.e., narrow) as Tokyo, the proposed model might not be very effective due to its dependence on satellite visibility. In this case, the proposed model needs to be retrained using more data in order to cover all viaduct scenarios. This does not mean that the proposed approach needs to retrain for every specific region and viaduct.

D. Overall Performance

Several data of the four driving scenarios are recorded to investigate the performance of the proposed methods. Fig. 14 shows the recognition rate of the proposed methods. Successful recognition is defined as $P(B_t = on)$ being larger than 50% if the vehicle is driving on the bridge and vice versa.

All methods can perfectly recognize if the vehicle is driving on the bridge. HMM using receiver-estimated height or SV do not perform well in the other three scenarios. On the other hand, the DBN-based methods have satisfactory performance, a more than 80% recognition rate in all scenarios. To further

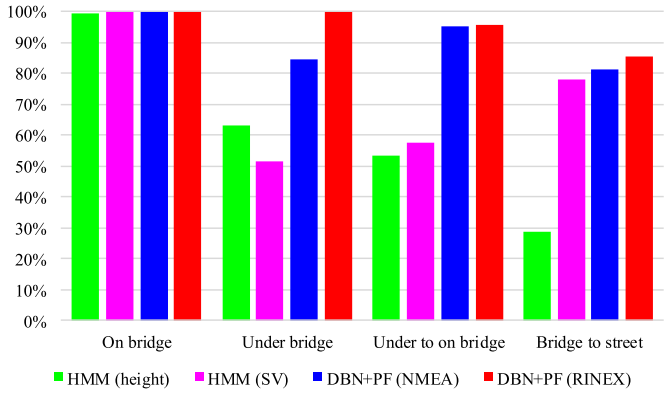

Fig. 14. Recognition rate of the proposed method in four typical driving scenarios in the vicinity of viaduct.

TABLE I
MEAN OF POSITIONING ERROR OF THE PROPOSED METHODS IN VERTICAL DIRECTION

	On bridge (m)	Under bridge (m)	Street to bridge (m)	Bridge to street (m)
GPS receiver height	2.45	11.94	35.78	13.27
DBN+PF (NMEA)	1.13	2.64	2.02	4.92
DBN+PF (RINEX)	1.54	2.45	1.79	3.34

TABLE II
PERFORMANCE OF DBN BASED ON RINEX USING DIFFERENT NUMBERS OF PARTICLES DISTRIBUTED BETWEEN 0 TO 100 METERS

Particle number	Recognition rate	Mean of height error	Std. of height error
On bridge			
2	87.82%	2.13 m	3.13 m
5	100%	1.07 m	1.24 m
10	100%	1.15 m	1.36 m
Under bridge			
2	53.4%	5.96 m	2.94 m
5	100%	2.06 m	2.08 m
10	100%	1.97 m	1.94 m
Under to on bridge			
2	88.11%	3.00 m	4.08 m
5	92.52%	2.15 m	3.29 m
10	92.52%	2.19 m	4.93 m
Bridge to street			
2	63.98%	5.13 m	6.14 m
5	95.77%	3.09 m	3.00 m
10	94.12%	3.44 m	3.27 m

improve the performance of the proposed method in transition driving exiting or entering a viaduct, an additional class (transition) could be added to decision B as {on, transition, under} in the proposed model. However, the data collection and labelling of the transition data are challenging. The performance of the DBN methods in estimating vehicle driving altitude is listed in Table I. DBN based on NMEA and RINEX measurements can obtain an accuracy of less than 5 and 3.5 meters in mean error,

respectively. In fact, the height difference between street and bridge is around 20 meters; 3.5 meter accuracy is supposed to be sufficient to distinguish driving on bridge from driving on street. Finally, similar to the conclusion obtained from Fig. 14, the more information (SV, NMEA and RINEX) that is used, the better the performance.

Moreover, the impact of different numbers of particles in the proposed DBN method using SV, NMEA and RINEX (Method 4) is evaluated. The result is listed in Table II. In general, the performance of the method using two particles is worse than that using five and ten. The performance of five and ten particles is very similar. Thus, we conclude that 5 particles is enough for the proposed DBN method.

V. Conclusions

Due to the density of the population in capital cities, the driving networks are more complicated than ever. Viaducts play an important part in the design of urban highways. They are used extensively in highly urbanized cities such as Tokyo, Hong Kong and Taipei. Current GNSS navigators suffer from signal blockage in the vicinity of the viaduct (bridge) area, resulting in erroneous determination of where the vehicle is driving, especially in terms of altitude direction. Based on the nature of signal blockage when driving "under" the viaduct, satellite visibility has the potential to indicate the scenario in which the vehicle is driving. This paper, therefore, first proposes a vehicle on-under bridge determination model based on the estimated vehicle height and satellite visibility. Due to the existence of discrete and continuous states, a DBN is designed and inferred by a SIR PF. According to the experiment result, the proposed method can successfully estimate the driving altitude of vehicles and determine the driving area in four typical scenarios. Overall, a more than 80% recognition rate can be achieved.

This paper proposes improving the on-under bridge determination ability of a standalone GPS navigator for advanced driver assistant systems. However, this technique can also be extended to the research field of probe data-based city development and traffic analysis.

References

[1] Y. K. Chen and T. G. Tsai, "GPS correction with the sky-subimage recognition," in *Proc. 7th Int. Conf. Digit. Inf. Manage.*, 2012, pp. 365–370.

[2] Y. K. Chen and T. H. Tsai, "Sky recognitions for driving-view images," in *Proc. 2013 IEEE Int. Conf. Veh. Electron. Saf.*, 2013, pp. 119–124.

[3] P. Jiang *et al.*, "Designing of viaduct automatic height limit device based on dual radio frequency recognition," in *Proc. 2016 3rd Int. Conf. Syst. Inf.*, 2016, pp. 627–632.

[4] J. Huang, X. Li, Y. Sun, and Q. Xu, "A highly-reliable combined positioning method for vehicle in urban complex environments," in *Proc. 2013 IEEE Int. Conf. Veh. Electron. Saf.*, 2013, pp. 153–158.

[5] M. Bevermeier, O. Walter, S. Peschke, and R. Haeb-Umbach, "Barometric height estimation combined with map-matching in a loosely-coupled Kalman-filter," in *Proc. 2010 7th Workshop Positioning, Navig. Commun.*, 2010, pp. 128–134.

[6] J. Park, D. Lee, and C. Park, "Implementation of vehicle navigation system using GNSS, INS, odometer and barometer," *J. Positioning, Navig., Timing*, vol. 4, no. 3, pp. 141–150, 2015.

[7] Y. Gu, L.-T. Hsu, and S. Kamijo, "Passive sensor integration for vehicle self-localization in urban traffic environment," *Sensors*, vol. 15, no. 12, pp. 30199–30220, 2015.

[8] S. Kamijo, Y. Gu, and L.-T. Hsu, "Autonomous vehicle technologies: localization and mapping," *IEICE Fundam. Rev.*, vol. 9, no. 2, pp. 131–141, Oct. 2015.

[9] B. W. Parkinson, "Differential GPS," in *Global Positioning System: Theory and Applications*, vol. 1, J. J. Spilker and B. W. Parkionson, Eds. Washington, DC, USA: AIAA, 1996, pp. 3–50.

[10] T. Takasu and A. Yasuda, "Development of the low-cost RTK-GPS receiver with an open source program package RTKLIB," presented at the *Int. Symp. GPS/GNSS 2009*, Jeju, South Korea, Nov. 2009.

[11] L.-T. Hsu, Y. Gu, Y. Huang, and S. Kamijo, "Urban pedestrian navigation using smartphone-based dead reckoning and 3D map-aided GNSS," *IEEE Sens. J.*, vol. 16, no. 5, pp. 1281–1293, Mar. 2016.

[12] E. D. Kaplan, *Understanding GPS: Principles and Application*, 1st ed. Boston, MA, USA: Artech House, 1996.

[13] F. Abdallah, G. Nassreddine, and T. Denoeux, "A multiple-hypothesis map-matching method suitable for weighted and box-shaped state estimation for localization," *IEEE Trans. Intell. Transp. Syst.*, vol. 12, no. 4, pp. 1495–1510, Dec. 2011.

[14] G. R. Jagadeesh, T. Srikanthan, and X. D. Zhang, "A map matching method for GPS based real-time vehicle location," *J. Navig.*, vol. 57, no. 3, pp. 429–440, 2004.

[15] H.-J. Chu, G.-J. Tsai, K.-W. Chiang, and T.-T. Duong, "GPS/MEMS INS data fusion and map matching in urban areas," *Sensors*, vol. 13, no. 9, pp. 11280–11288, 2013.

[16] M. A. Quddus, W. Y. Ochieng, and R. B. Noland, "Current map-matching algorithms for transport applications: State-of-the art and future research directions," *Transp. Res. Part C: Emerging Technol.*, vol. 15, no. 5, pp. 312–328, 2007.

[17] G. R. Jagadeesh and T. Srikanthan, "Heuristic optimizations for high-speed low-latency online map matching with probabilistic sequence models," in *Proc. 2016 IEEE 19th Int. Conf. Intell. Transp. Syst.*, 2016, pp. 2565–2570.

[18] I. Szottka, "Particle filtering for lane-level map-matching at road bifurcations," in *Proc. 16th Int. IEEE Conf. Intell. Transp. Syst.*, 2013, pp. 154–159.

[19] P. Bender, J. Ziegler, and C. Stiller, "Lanelets: Efficient map representation for autonomous driving," in *Proc. 2014 IEEE Intell. Veh. Symp.*, 2014, pp. 420–425.

[20] J. Rabe, M. Meinke, M. Necker, and C. Stiller, "Lane-level map-matching based on optimization," in *Proc. 2016 IEEE 19th Int. Conf. Intell. Transp. Syst.*, 2016, pp. 1155–1160.

[21] M. Haklay and P. Weber, "OpenStreetMap: User-generated street maps," *IEEE Pervasive Comput.*, vol. 7, no. 4, pp. 12–18, Oct./Dec. 2008.

[22] S. Peyraud *et al.*, "About non-line-of-sight satellite detection and exclusion in a 3D map-aided localization algorithm," *Sensors*, vol. 13, no. 1, pp. 829–847, 2013.

[23] D. Betaille, F. Peyret, M. Ortiz, S. Miquel, and L. Fontenay, "A new modeling based on urban trenches to improve GNSS positioning quality of service in cities," *IEEE Intell. Transp. Syst. Mag.*, vol. 5, no. 3, pp. 59–70, Fall 2013.

[24] C. Fouque and P. Bonnifait, "Multi-hypothesis map-matching on 3D navigable maps using raw GPS measurements," in *Proc. 13th Int. IEEE Conf. Intell. Transp. Syst.*, 2010, pp. 1498–1503.

[25] P. D. Groves, "Shadow matching: A new GNSS positioning technique for urban canyons," *J. Navig.*, vol. 64, no. 3, pp. 417–430, 2011.

[26] L. Wang, P. D. Groves, and M. K. Ziebart, "Smartphone shadow matching for better cross-street GNSS positioning in urban environments," *J. Navig.*, vol. 68, no. 3, pp. 411–433, May 2015.

[27] R. Yozevitch, B. Ben-Moshe, and A. Dvir, "GNSS accuracy improvement using rapid shadow transitions," *IEEE Trans. Intell. Transp. Syst.*, vol. 15, no. 3, pp. 1113–1122, Jun. 2014.

[28] M. Obst, S. Bauer, P. Reisdorf, and G. Wanielik, "Multipath detection with 3D digital maps for robust multi-constellation GNSS/INS vehicle localization in urban areas," in *Proc. 2012 IEEE Intell. Veh. Symp.*, 2012, pp. 184–190.

[29] S. Miura, L. T. Hsu, F. Chen, and S. Kamijo, "GPS error correction with pseudorange evaluation using three-dimensional maps," *IEEE Trans. Intell. Transp. Syst.*, vol. 16, no. 6, pp. 3104–3115, Dec. 2015.

[30] T. Suzuki and N. Kubo, "Correcting GNSS multipath errors using a 3D surface model and particle filter," in *Proc. 26th Int. Tech. Meeting Satell. Div. Inst. Navig.*, Nashville, TN, USA, 2013, pp. 1583–1595.

[31] L.-T. Hsu, Y. Gu, and S. Kamijo, "3D building model-based pedestrian positioning method using GPS/GLONASS/QZSS and its reliability calculation," *GPS Solutions*, vol. 20, no. 3, pp. 413–428, 2016.

[32] Y. Gu, L.-T. Hsu, and S. Kamijo, "GNSS/on-board inertial sensor integration with the aid of 3D building map for lane-level vehicle self-localization in urban canyon," *IEEE Trans. Veh. Technol.*, vol. 65, no. 6, pp. 4274–4287, Jun. 2015.
[33] J. Breßler, P. Reisdorf, M. Obst, and G. Wanielik, "GNSS positioning in non-line-of-sight context–A survey," in *Proc. 2016 IEEE 19th Int. Conf. Intell. Transp. Syst.*, 2016, pp. 1147–1154.
[34] V. Pavlovic, B. J. Frey, and T. S. Huang, "Time-series classification using mixed-state dynamic Bayesian networks," in *Proc. IEEE Comput. Soc. Conf. Comput. Vis. Pattern Recog.*, vol. 2, 1999, pp. 1–615.
[35] P. Misra and P. Enge, *Global Positioning System: Signals, Measurements, and Performance*. Lincoln, MA, USA: Ganga-Jamuna Press, 2011.
[36] N. Kubo, R. Kikuchi, and M. Higuchi, "A unique approach to strong multipath mitigation in dense urban areas," in *Proc. Inst. Navig. GNSS+ 2015*, Tampa, FL, USA, 2015, pp. 2905–2913.
[37] N. Kubo, K. K., L.-T. Hsu, and O. Amai, "Multipath mitigation technique under strong multipath environment using multiple antennas," *J. Aeronaut., Astronaut. Aviation, Ser. A*, vol. 49, no. 1, pp. 75–82, 2017.
[38] M. G. Petovello and P. D. Groves, "Multipath vs. NLOS signals," *Inside GNSS*, vol. 8, no. 6, pp. 40–42, 2013.
[39] N. M. Drawil, H. M. Amar, and O. A. Basir, "GPS localization accuracy classification: A context-based approach," *IEEE Trans. Intell. Transp. Syst.*, vol. 14, no. 1, pp. 262–273, Mar. 2013.
[40] A. J. Dobson and A. Barnett, *An Introduction to Generalized Linear Models*. New York, NY, USA: Chapman and Hall/CRC, 2008.
[41] L. T. Hsu, H. Tokura, N. Kubo, Y. Gu, and S. Kamijo, "Multiple faulty GNSS measurement exclusion based on consistency check in urban canyons," *IEEE Sens. J.*, vol. 17, no. 6, pp. 1909–1917, Mar. 2017.
[42] A. Doucet, S. Godsill, and C. Andrieu, "On sequential Monte Carlo sampling methods for Bayesian filtering," *Statist. Comput.*, vol. 10, no. 3, pp. 197–208, 2000.
[43] W. Gurtner, "Innovation: Rinex–the receiver independent exchange format," *GPS World*, vol. 5, no. 7, pp. 48–53, 1994.
[44] N. M. E. Association, *NMEA 0183–Standard for Interfacing Marine Electronic Devices*. San Jose, CA, USA: NMEA, 2002.

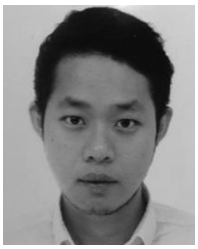

Li-Ta Hsu (S'09–M'15) received the B.S. and Ph.D. degrees in aeronautics and astronautics from the National Cheng Kung University, Tainan, Taiwan, in 2007 and 2013, respectively.

He is currently an Assistant Professor with the Interdisciplinary Division of Aeronautical and Aviation Engineering, Hong Kong Polytechnic University, Hong Kong; previously, he served as a Post-Doctoral Researcher with the Institute of Industrial Science, University of Tokyo, Tokyo, Japan. In 2012, he was a Visiting Scholar with the Faculty of Engineering, University College London, London, U.K. His research interests include GNSS positioning in challenging environments and localization for autonomous driving vehicles and unmanned aerial vehicles.

Yanlei Gu (M'14) received the M.E. degree from Harbin University of Science and Technology, Harbin, China, in 2008, and the Ph.D. degree in computer science from Nagoya University, Nagoya, Japan, in 2012.

He has been a Post-Doctoral Researcher with the Institute of Industrial Science, University of Tokyo, Tokyo, Japan, since 2013. His research interests include computer vision and machine learning and their applications to ITS. He is a member of the IEEE ITS Society. He has served as the organizing committee member for IEEE ICVES2015 and ITSC2017.

Shunsuke Kamijo (M'97) received the B.S. and M.S. degrees in physics and the Ph.D. degree in information engineering from the University of Tokyo, Tokyo, Japan, in 1990, 1992, and 2001, respectively.

He began working for Fujitsu Ltd. in 1992 as a Processor Design Engineer. He was an Assistant Professor from 2001 to 2002 and has been an Associate Professor since 2002. His research interests include computer vision, wireless communication, and their applications to ITS. His research focuses are autonomous vehicles, traffic video surveillance, traffic signal control, V2X communications, and pedestrian and car navigations.

Dr. Kamijo is a member of the IEEE ITS Society, TRB, IEICE, and IATSS. He joined the International Program Committee of ITS World Congress in 2011. He has been a member of the Board of Governors of the IEEE ITS Society since 2015 and an Executive Committee member of the society since 2017. He has served as the Vice-Chairman of the program committee for the ITS World Congress Tokyo 2013, the General Co-Chair for IEEE ICVES2015 and ITSC2017, and the International Program Chair for IEEE IV2017. He is an editorial board member of the *International Journal on ITS Research* and *Multimedia Tools and Applications*.